Journal of Wind Engineering & Industrial Aerodynamics 224 (2022) 104987

Contents lists available at ScienceDirect

Journal of Wind Engineering & Industrial Aerodynamics

journal homepage: www.elsevier.com/locate/jweia

Impact of the train-track-bridge system characteristics in the runnability of high-speed trains against crosswinds - Part II: Riding comfort

P.A. Montenegro [a,*], D. Ribeiro [b], M. Ortega [c,d], F. Millanes [c,d], J.M. Goicolea [d], W. Zhai [e], R. Calçada [a]

[a] CONSTRUCT, LESE, Faculty of Engineering, University of Porto, Rua Dr. Roberto Frias s/n, 4200-465, Porto, Portugal
[b] CONSTRUCT, LESE, School of Engineering, Polytechnic of Porto, Rua Dr. António Bernardino de Almeida 431, 4249-015, Porto, Portugal
[c] IDEAM, SA, Calle Jorge Juan, 19 – 3°, 28001, Madrid, Spain
[d] School of Civil Engineering, Technical University of Madrid, Calle del Prof. Aranguren, 3, 28040, Madrid, Spain
[e] Train and Track Research Institute, State Key Laboratory of Traction Power, Southwest Jiaotong University, 610031, Chengdu, China

ARTICLE INFO

Keywords:
Passenger riding comfort
Continuous and mean comfort
Sperling index
Train-track-bridge interaction
High-speed railway bridges
Wind loads

ABSTRACT

Passenger riding comfort is a major concern in railways, particularly in high-speed (HS) networks due its strict requirements. Both the track and vehicle conditions may influence the comfort experienced by the passengers, but other external factors may also do it. Among these factors, the effects caused by crosswinds stand out due to the high levels of vibrations that may cause to the vehicle. However, almost no studies in this regard can be found in the literature, since most of the works do not consider external loads and do not analyse this phenomenon on bridges. Thus, the present work aims to fill this gap, by evaluating the passenger comfort on bridges subjected to crosswinds with different lateral structural behaviours and track conditions. Based on the vehicle's accelerations computed with an in-house dynamic train-track-bridge interaction tool, the Mean and Continuous comfort indexes defined by the European norm EN 12299, as well as the Sperling index, have been assessed for distinct scenarios. The bridge's lateral behaviour shows a negligible effect in the riding comfort, as well as the track quality since the wind load is much more determinant for the carbody vibrations than the track irregularities considered in this work.

1. Introduction

High-speed (HS) railways became, in the last decades, one of the most successful means of transport for medium and long distances. Countries such as China, for example, proved that HS railways are very efficient and popular not only in small and medium size countries, but also in regions with continental size, making it a strong competitor with air transport. Moreover, the lower environmental impact associated with railway transport is leading to a significant increase of both public and private investments in this area. Nonetheless, the relatively long journey times lead to a greater demand from passengers in terms of riding comfort. While comfort is not a significant issue in short daily commutes, long trips, both in tourism and professional contexts, must follow strict riding comfort requirements.

Riding comfort is associated with several factors such as the ambient temperature inside the carbody, noise, humidity, smell, vibration, among others. The vibrations felt by the passengers are one of the most important sources of discomfort among passengers, since they could cause them fatigue and, in some situations, lead to resonance of internal organs and consequent motion sickness (Kumar et al., 2017). However, it is a very complicated phenomenon since it may be dependent on a significant number of factors, namely the infrastructure condition, the vehicle's characteristics (suspensions, existence of wheel defects, etc) and external sources of excitation, such as rain, snow or wind. Regarding the latter, it is particularly important in railway lines with a significant percentage of bridges and viaducts, since this type of infrastructure is generally more prone to crosswinds due to the high elevations of decks and locations in deep valleys. Therefore, studying the implications of the vibrations felt inside a vehicle in the passenger riding comfort is a topic of utmost interest that is addressed nowadays on several codes, such as EN 12299 (2009) and GB/T 5599-2019 (2019). However, the study of comfort when trains cross bridges subjected to crosswinds is still an

* Corresponding author..
E-mail addresses: paires@fe.up.pt (P.A. Montenegro), drr@isep.ipp.pt (D. Ribeiro), miguel.ortega@ideam.es (M. Ortega), francisco.millanes@ideam.es (F. Millanes), jose.goicolea@upm.es (J.M. Goicolea), wmzhai@home.swjtu.edu.cn (W. Zhai), ruiabc@fe.up.pt (R. Calçada).

https://doi.org/10.1016/j.jweia.2022.104987
Received 13 October 2021; Received in revised form 3 February 2022; Accepted 30 March 2022
Available online 19 April 2022

under-discussed topic among the scientific community that deserves special attention, particularly due to the increasing percentage of viaducts in the newer HS railway lines (Montenegro et al., 2021).

To numerically study the riding comfort related with the vibrations of the carbody, complex dynamic train-track-bridge interaction (TTBI) models have to be used to assess the vehicle's response (Antolin et al., 2012; Zhai et al., 2019; Xiang et al., 2020). Most of the works addressing the train behaviour on bridges in the presence of strong lateral winds are related with the train running safety (Guo et al., 2013; Montenegro et al., 2020a; Wang et al., 2021, 2022) and not with the riding comfort. To the authors knowledge, only a few recent exceptions can be found in the literature but without being focused exclusively on the passenger comfort. Guo et al. (2007) performed a numerical simulation of the dynamic performance of a HS train running over the Tsing Ma suspension bridge in Hong Kong considering the wind data obtained during the passage of a typhoon (Xu et al., 2007). In this study, the authors concluded that both the safety and comfort levels were in an acceptable level when the train crossed the bridge at low speeds (around 100 km/h). However, no conclusions have been drawn regarding the train's behaviour under other situations, such as different speeds, different wind loads or different conditions of the bridge itself. He et al. (2017) established a rigid-flexible approach to study the dynamic behaviour of a train-bridge system subjected to wind loads. In this model, the authors coupled the rigid model of a train developed with a multibody dynamics software with a flexible finite element (FE) model of the Xijiang HS railway bridge in China. The authors analysed the dynamic performance of the train in terms of running safety and riding comfort, but the calculations were restricted first to a single train speed (200 km/h) and then to a single wind velocity (20 m/s). Therefore, only the critical wind and train speeds for these two specific situations were obtained, which limited the scope of the conclusions. Olmos and Astiz (2018) studied the effects of crosswinds in a HS train moving over a high-pier viaduct in Spain. They evaluated the influence of two types of countermeasures, namely wind barriers and tuned mass dampers, in the derailment risk and riding comfort. They conclude that wind barriers are strongly effective to control both problems, while the TMDs only slightly improve the running safety. However, like the previous study, only one particular bridge was studied and the comfort was evaluated exclusively with a single comfort index, making the conclusions less generic.

On the other hand, the few studies that focus exclusively on the passenger riding comfort considering the vehicle vibrations are not related with the performance of trains running over bridges in the presence of crosswinds. Kumar et al. (2017) developed a flexible model of an Indian train which incorporates several human biodynamic models developed with lumped mass elements, that represent the human body parts, connected through spring-dashpots. By considering simplified periodic irregularities as the main source of excitation, the authors conducted a series of dynamic analyses and evaluated the riding comfort through the Sperling index. It was concluded that the values of the Sperling index were not significantly affected when the flexible modes of the carbody were considered, i.e., the results were practically the same when only the rigid body modes of the carbody were considered in the analysis. Moreover, the acceleration responses obtained at the different body parts using the biodynamic model were slightly overestimated when the flexible modes were neglected, but only for train speeds above 80 km/h. Dumitriu and Leu (2017) presented a correlation between the Sperling index and the Mean Comfort index stipulated by the European norm EN 12299 (2009). Then, the authors developed a two-dimensional rigid body model of a railway vehicle and compared the comfort indexes considering only the vertical acceleration responses. They noticed that both indexes tend to increase with increasing speeds, but not uniformly, due to the geometric filtering effects that affects the vehicle's vertical vibrations (Gong et al., 2013). Jiang et al. (2019) performed a more comprehensive comparison between the Sperling and European comfort indexes using on-board acceleration measurements from a passenger wagon from the Australian V/Line transport operator. The tests were conducted on 267 km long railway test line with a peak operating speed of 120 km/h. Although the Mean Comfort index (EN 12299, 2009) takes into consideration the effects on all directions, the authors analysed it separately for each direction and proposed fitting curves to correlate them with the Sperling indexes. At the end, the authors also proposed the so-called compound Sperling index, which comprehends the effects of the vibrations measured in the three directions, making it more comparable with the normative Mean Comfort index. More recently, Deng et al. (2021) carried out an exhaustive study of the Sperling index using different algorithms and pointed that, different approaches may lead to different comfort levels, even when using the same evaluation index.

All the aforementioned studies have at least one of the following drawbacks regarding the comfort evaluation in the presence of wind: i) study of a single bridge with a single index; ii) in the presence of winds, the major focus is always on running safety; iii) the works that put more emphasis on the riding comfort, do not consider flexible structures and wind loads. Hence, the present paper aims to fill these gaps by establishing a comprehensive study that assesses the influence of several different factors, such as bridge's flexibility, track quality and type of comfort index, in the riding comfort of trains against crosswinds. To achieve this goal, the following three major objectives are set:

- Objective 1: analysis of the influence of the bridge lateral response in the passenger riding comfort against crosswinds. Like in the Part I of this paper (Montenegro et al., 2022) dedicated to the train running safety, the Arroyo de Las Piedras viaduct is used as the main case study, being then parametrized in relation to its lateral flexibility to check if it influences the riding comfort or not.
- Objective 2: assess the impact of the track condition in the riding comfort considering different wind loads. Different track irregularity profiles are considered together with the different wind loads and train speeds.
- Objective 3: compare the results using the European method stipulated by EN 12299 (2009) (Mean and Continuous Comfort indexes) with the Sperling indexes adopted, for example, by the Chinese norm GB/T 5599-2019 (2019). Unlike some of the cited works, the present work makes a comprehensive analysis of the differences between the two methods, taking into consideration the different frequencies of interest, weighting functions, etc.

In Part I of the paper (Montenegro et al., 2022), an additional objective related with the influence of the axle weight of different trains in the traffic stability was also addressed. However, unlike the running safety, the riding comfort may be strongly dependent on several properties of the vehicle, such as suspension properties, geometry, weight, etc. Therefore, given the huge variability in the different train properties, this Part II does not takes into consideration different vehicles, focusing only on the AVE-S103 HS train. Thus, several TTBI dynamic analyses have been conducted to assess the acceleration responses inside the carbody considering a wide range of scenarios defined by different wind velocities, train speeds, track conditions and structural lateral flexibilities.

2. Methodology to evaluate the passenger riding comfort on bridges

2.1. Overview

The passenger comfort can be influenced by several factors, such as temperature, noise and vibrations. Although all these factors may significantly affect the comfort feeling of the passengers, only the latter will be addressed in this work, since it is the only one related to the mechanical behaviour of the train and that can be simulated with TTBI dynamic analysis. Although comfort does not represent a limit state related with safety, its importance is critical, particularly in long journeys, to avoid unpleasant feelings in the passengers for a long time.

Normatively, the comfort related to vibrations of the carbody transmitted to the human body is addressed in the European norm EN 12299 (2009) and in the Chinese norm GB/T 5599-2019 (2019). According to the former, riding comfort in railways can be defined as a complex sensation produced on the passenger by the carbody motions of the railway vehicle and transmitted to the body through the interfaces. In the present work, the Mean and Continuous Comfort indexes defined in EN 12299 (2009) and the Sperling index adopted by GB/T 5599-2019 (2019) are used to assess the passenger riding comfort in the presence of crosswinds. The remaining methods stipulated by the European norm, namely, to analyse comfort in transition curves and during discrete

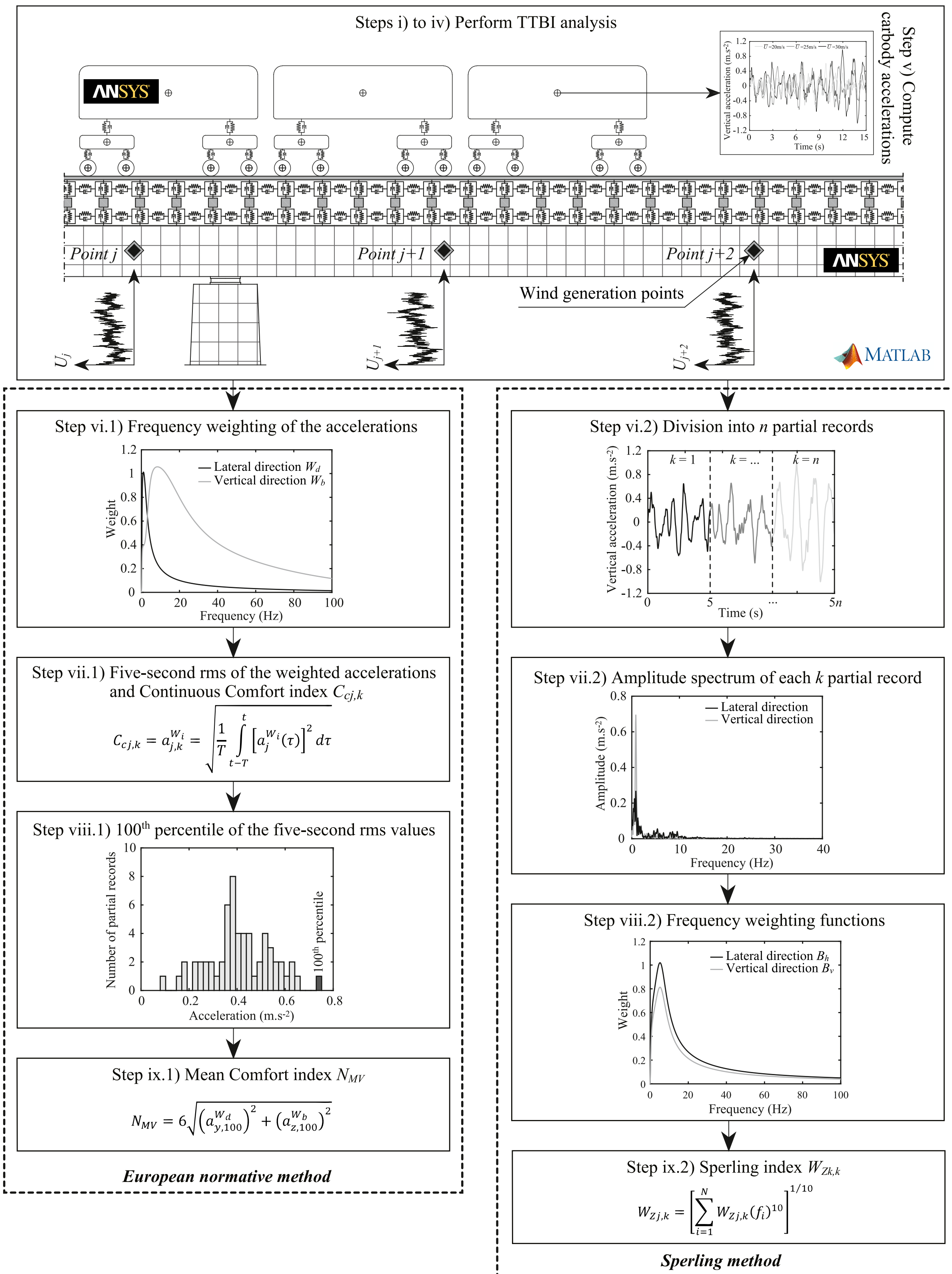

Fig. 1. Framework of the methodology to assess the passenger riding comfort on bridges subjected to crosswinds using a TTBI tool.

events, are not addressed here because the HS railway viaducts are generally straight or with very large curve radius and the discrete events mentioned by the norm are related with local track defects, which is out of the scope of this work. To compute these indexes in scenarios where a HS train crosses a bridge subjected to crosswinds, the numerical methodology based on a TTBI tool schematized in Fig. 1 is used. It is composed by five general steps, in which the first four coincide with those presented in the framework of the methodology described in Part I to assess running safety (Montenegro et al., 2022). They are (see Fig. 1):

i. Development of numerical models: the numerical models of the railway vehicle and track-bridge system are developed in a FEM package.
ii. Definition of the wind load: the wind velocity fields are generated through an ergodic stochastic process. Then, the wind velocities are converted into loads through the quasi-steady theory corrected with a weighting function.
iii. Data import: the structural matrices of the numerical models developed in step i) and the vectors of wind forces acting on the bridge and train computed in step ii) are imported by the TTBI tool written in MATLAB® (2018).
iv. Perform TTBI dynamic analysis: the TTBI tool couples the train-track-bridge system, applies the wind aerodynamic forces to the system and performs the dynamic analysis.
v. Computation of the vertical and lateral acceleration response of the carbody: the time-histories of the vertical and lateral accelerations in the carbody are obtained from the analyses to be later manipulated.

Then, depending on the method to assess the passenger comfort, four additional steps have to be followed, namely vi.1 to ix.1 for the European method (EN 12299, 2009) and vi.2 to ix.2 for the Sperling method (GB/T 5599-2019, 2019).

2.2. Comfort evaluation according to the European norm

2.2.1. Frequency weighting functions

After computing the acceleration responses, as described in step v) described in the previous section, the records are frequency weighted to consider the frequency ranges that most affect the human comfort (step vi.1 from Fig. 1). Since the human body responds differently to each direction of vibration, the weighting functions W_i are different depending on that direction ($i = d, b$ for the lateral and vertical directions, respectively). According to EN 12299 (2009), the weighting function for the lateral direction $W_d(f)$ is expressed as a product of several transfer functions as

$$W_d(f) = H_h(f).H_l(f).H_t(f) \tag{1}$$

while the weighting function relative to the vertical direction $W_b(f)$ is given by

$$W_b(f) = H_h(f).H_l(f).H_t(f).H_s(f) \tag{2}$$

where $H_h(f)$, $H_l(f)$, $H_t(f)$ and $H_s(f)$ are the high-pass, low-pass, acceleration to velocity transition (*a*-*v*) and upward gradient transfer functions, respectively, that can be consulted in the Annex C from EN 12299 (2009).

Fig. 2 presents the frequency weighting curves associated with the lateral $W_d(f)$ and vertical $W_b(f)$ weighting functions, where it is possible to observe the frequency range to which the humans are most sensitive to the vertical vibrations (4–16.5 Hz) is much wider than that relative to the lateral ones (0.6–2 Hz). A more detailed description on the origin of these curves based on the experiments carried out for the development of the precursor normative ISO 2631-4 (2001) can be found in Knothe and Stichel (2017).

2.2.2. Continuous Comfort index

The Continuous Comfort index $C_{cj,k}$ aims to take into account the short time effects on the human body when it is exposed to vibrations measured on the carbody's floor (step vii.1 from Fig. 1). This index is evaluated separately to each direction j and consists of the 5-s weighted rms-values of the accelerations $a_{j,k}^{W_i}$ (in m/s^2) used to assess the Mean Comfort index. Considering a direction j, the kth 5-s rms-value of the weighted acceleration is given by

$$C_{cj,k} = a_{j,k}^{W_i} = \sqrt{\frac{1}{T}\int_{t-T}^{t}\left[a_j^{W_i}(\tau)\right]^2 d\tau} \tag{3}$$

where T is equal to 5 s and t is a multiple of 5 s. Thus, the Continuous Comfort index is evaluated for each interval of 5 s indicated by k. The scale for the Continuous Comfort index for all directions is presented in Table 1.

2.2.3. Mean Comfort index

For the evaluation of the Mean Comfort index through the Standard Method described in EN 12299 (2009), the 95th percentile of the distributions of 5-s weighted rms-values $a_{j,95}^{W_i}$ over a period of 5 min ($n = 60$)

Table 1
Scale for the Continuous Comfort index $C_{cj,k}$ (EN 12299, 2009).

Ranges of $C_{cj,k}$ (m/s^2)	Comfort sensitivity
$C_{cj,k} < 0.20$	Very comfortable
$0.20 \le C_{cj,k} < 0.30$	Comfortable
$0.30 \le C_{cj,k} < 0.40$	Medium
$C_{cj,k} \ge 0.40$	Less comfortable

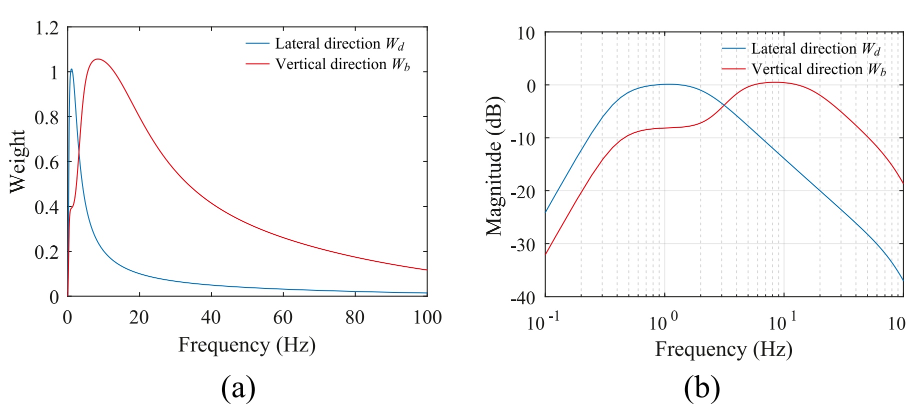

Fig. 2. Frequency weighting curves according to EN 12299 (2009): (a) weighting factor and (b) magnitude.

should be considered. However, since the focus of this work is on the assessment of the riding comfort of HS trains running over bridges, the time period, i.e., the time required for the train to cross the bridge, is usually much less than 5 min. To overcome this issue, and to guarantee a conservative result, the 100th percentile of the 5-s weighted rms-values $a_{j,100}^{W_i}$ has been adopted to calculate the Mean Comfort index instead of the 95th, i.e., independently of the number of partial records obtained in each analysis (lower speeds lead to longer analysis and to a higher number of 5-s partial records, and vice-versa), the highest rms-value for each direction is adopted (step viii.1 from Fig. 1). Thus, knowing that the rms-value corresponding to the longitudinal x direction is neglected given the constant train speed assumed in this work, the Mean Comfort index N_{MV} is expressed as (step ix.1 from Fig. 1)

$$N_{MV} = 6\sqrt{\left(a_{y,100}^{W_d}\right)^2 + \left(a_{z,100}^{W_b}\right)^2} \tag{4}$$

A more complex method, called Mean Comfort Complete Method is also described in EN 12299 (2009) that considers not only the acceleration records measured on the carbody's floor, but also on the seat pan and back. However, a more complete vehicle model considering the local passenger-seat dynamic system, such as those developed by Ribeiro et al. (2012) and Meixedo et al. (2014), would be necessary. Moreover, according to EN 12299 (2009), the Standard Method is perfectly acceptable for situations where the longitudinal vibrations are not excessive, which is in accordance with typical HS journeys, where the train speeds tend to be constant due to the large radius of the curves and few number of stops. The scale for the Mean Comfort index is presented in Table 2.

2.3. Comfort evaluation according to the sperling index

2.3.1. Frequency weighting functions

After dividing the acceleration responses into n 5-s partial records (step vi.2 from Fig. 1) and calculating the amplitude spectrum of each of those records (step vii.2 from Fig. 1), it is necessary to compute the frequency weighting functions (step viii.3 from Fig. 1). Based on vibration tests in humans, the weighting function from the Sperling index $F(f)$ is defined through Table 3.

According to Knothe and Stichel (2017) and Jiang et al. (2019), an alternative, but similar, weighting function for the lateral direction $B_h(f)$ is more commonly used nowadays

$$B_h(f) = 0.737\sqrt{\frac{1.911f^2 + \left(0.25f^2\right)^2}{\left(1 - 0.277f^2\right)^2 + \left(1.564f - 0.0368f^3\right)^2}} \tag{5}$$

while for the vertical direction, the function $B_v(f)$ can be expressed as a function of the previous one through

$$B_v(f) = 0.798B_h(f) \tag{6}$$

Fig. 3 presents the weighting functions associated with the lateral $B_h(f)$ and vertical $B_v(f)$ directions. In this work, although very similar, the Sperling index is computed with both weighting functions $B(f)$ and $F(f)$ and the most conservative values are adopted. Contrary to the filters specified by EN 12299 (2009), the sensitive ranges in the Sperling index are the same for the lateral and vertical directions (3–7 Hz). The differences in these sensitivity ranges are explained by the fact the relationship between the sensitivity of the human body and the frequency of vibration is not linear and straightforward. Thus, according to Jiang et al. (2019), frequency weighting curves are important to account for comfort from exposure to a wide range of frequencies, resulting in differences in the frequency weighting curves adopted in each ride comfort evaluation method.

Table 2
Scale for the Mean Comfort index N_{MV}.

Ranges of N_{MV}	Comfort sensitivity
$N_{MV} < 1.5$	Very comfortable
$1.5 \le N_{MV} < 2.5$	Comfortable
$2.5 \le N_{MV} < 3.5$	Medium
$3.5 \le N_{MV} < 4.5$	Uncomfortable
$N_{MV} \ge 4.5$	Very uncomfortable

Table 3
Sperling index's weighting function $F(f)$ for harmonic vibrations (GB/T 5599-2019, 2019).

Vertical vibration		Lateral vibration	
f (Hz)	$F(f)$	f (Hz)	$F(f)$
$0.5 \le f < 5.9$	$0.325f^2$	$0.5 \le f < 5.4$	$0.8f^2$
$5.9 \le f < 20.0$	$400/f^2$	$5.4 \le f < 26.0$	$650/f^2$
$f \ge 20.0$	1	$f \ge 26.0$	1

2.3.2. Sperling index

The Sperling index is currently adopted by the Chinese norm GB/T 5599-2019 (2019) to classify the riding comfort. For each direction j and 5-s record k, the Sperling index $W_{Zj,k}(f_i)$ for each frequency f_i can be expressed as

$$W_{Zj,k}(f_i) = 3.57\left[\frac{a_{j,k}(f_i)^3}{f_i}F(f_i)\right]^{1/10} \tag{7}$$

where $a_{j,k}(f_i)$ is the amplitude spectrum from the 5-s acceleration record k in the direction j (in m/s^2) and $F(f_i)$ is the frequency weighting function related with the human sensitivity to vibration defined in Table 3, both evaluated at the frequency f_i. Alternatively, the Sperling index for each frequency f_i can also be obtained based on the modified frequency weighting functions $B(f)$ defined in Eqs. (5) and (6) as (acceleration amplitude in m/s^2)

$$W_{Zj,k}(f_i) = 3.98\left[a_{j,k}(f_i)^3 \cdot B(f_i)^3\right]^{1/10} \tag{8}$$

Independently on the approach, the Sperling index $W_{Zj,k}$ related with the kth 5-s acceleration record in the direction j is computed over the entire interval of frequencies of interest through the following equation (step ix.2 from Fig. 1):

$$W_{Zj,k} = \left[\sum_{i=1}^{N} W_{Zj,k}(f_i)^{10}\right]^{1/10} \tag{9}$$

where N is the total number of discrete frequencies considered within the interval of interest. According to some authors (Dumitriu and Leu, 2017; Jiang et al., 2019), this interval should be between 0.5 Hz and 30 Hz, while the Chinese norm GB/T 5599-2019 (2019) points to the same lower bound but to a higher bound of 40 Hz. In the present work, to follow the normative specifications, the latter range is adopted.

To conclude, it is important to notice that the Sperling index is evaluated continuously for each 5-s interval k and for each direction j separately, similarly to the Continuous Comfort index discussed before within the European norm. Table 4 presents the two available scales for the Sperling index, namely one found in the literature (Dumitriu and Leu, 2017; Jiang et al., 2019; Deng et al., 2021) and another specified in the norm GB/T 5599-2019 (2019). Since the former is more discretized and similar to the Continuous Comfort index scale, it has been adopted in this work to evaluate the riding comfort through the Sperling index.

3. Train-track-bridge interaction model subjected to wind loads

The present section aims to give a global overview of the numerical model used to analyse the vehicle's behaviour against crosswinds and its interaction with the track-bridge sub-system. Since the detailed description of each of these sub-systems, as well as the wind model, is already presented in the Part I of this paper (Montenegro et al., 2022),

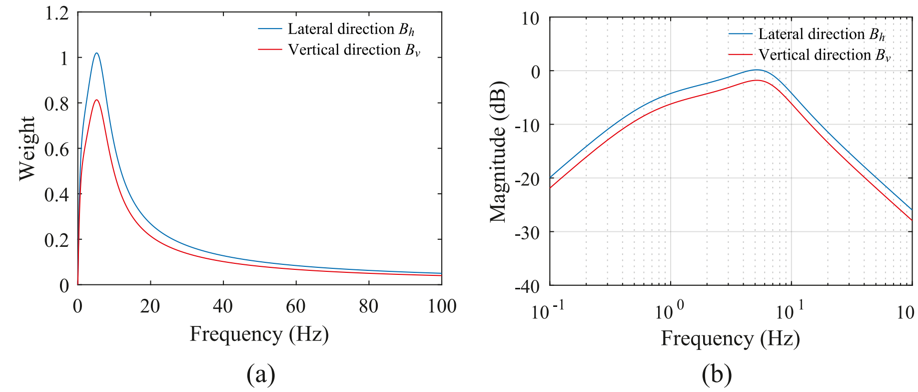

Fig. 3. Frequency weighting functions according to the Sperling index: (a) weighting factor and (b) magnitude.

Table 4
Scale for the Sperling index $W_{Zj,k}$.

Ranges of $W_{Zj,k}$	Comfort sensitivity	
	According to literature (Dumitriu and Leu, 2017; Jiang et al., 2019; Deng et al., 2021)	According to the Chinese norm GB/T 5599-2019 (2019)
$W_{Zj,k} < 1.0$	Just noticeable	Excellent
$1.0 \leq W_{Zj,k} < 2.0$	Clearly noticeable	
$2.0 \leq W_{Zj,k} < 2.5$	More pronounced, but not unpleasant	
$2.5 \leq W_{Zj,k} < 2.75$	Strong, irregular, but still tolerable	Good
$2.75 \leq W_{Zj,k} < 3.0$		Qualified
$3.0 \leq W_{Zj,k} < 3.25$	Very irregular	Poor
$3.25 \leq W_{Zj,k} < 3.5$	Extremely irregular, unpleasant, annoying; prolonged exposure intolerable	
$W_{Zj,k} \geq 3.5$	Extremely unpleasant; prolonged exposure harmful	

only a brief summary is given.

3.1. Wind model

The wind model adopted in this work consists of a stochastic formulation initially proposed by Cao et al. (2000) to be used in the particular case of bridges. The wind is applied to the bridge in the wind generation points equally spaced by 16 m, while an interpolation of the wind velocity field is performed to define the wind loads acting on the train. This interpolation is both spatial and temporal, since the variable position of the train may not coincide with the location of the wind generation points and the timesteps of the dynamic analysis are different from those used to define the wind velocity profiles. The fluctuating components of the wind field at the generation point j in the horizontal $u_j(t)$ and vertical $w_j(t)$ directions are stochastically generated as (see Part I for details)

$$u_j(t) = \sqrt{2\,\Delta\omega}\sum_{m=1}^{j}\sum_{f=1}^{N}\sqrt{S_u(\omega_{mf})}G_{jm}(\omega_{mf})\cos(\omega_{mf}t + \varphi_{mf}) \tag{10}$$

$$w_j(t) = \sqrt{2\,\Delta\omega}\sum_{m=1}^{j}\sum_{f=1}^{N}\sqrt{S_w(\omega_{mf})}G_{jm}(\omega_{mf})\cos(\omega_{mf}t + \varphi_{mf}) \tag{11}$$

where t is the time, φ_{mf} are random phase angles uniformly distributed in the interval $[0, 2\pi]$, $\Delta\omega$ is the frequency increment, N is the number of discrete frequencies used to generate the wind profile, S_u and S_v are the horizontal and vertical wind spectra, respectively, ω_{mf} is a modified frequency value given in Cao et al. (2000), and G_{jm} is an element of a coefficient matrix also described in Cao et al. (2000), which arises from the cross-spectral density matrix that correlates the wind spectra from all generation points. Given the stochastic characteristics of this generation process, the wind load that hits the train is different throughout the entire time-series of the wind velocity field. Therefore, to ensure a conservative analysis, it is assumed that the train crosses the wind generation point located at the middle of the bridge's deck (zone subjected to larger lateral movements) at the precise moment where the peak wind velocity from that particular wind time-series occurs (time series of 10 min, as explained in Part I). A detailed description of this procedure to select the critical stretch of the wind time-series can be found in Montenegro et al. (2020b).

With the wind velocity fields stochastically simulated, it is possible to compute the wind loads applied to the bridge through the following equation (see Part I for details)

$$F_{f,j}(t) = \frac{1}{2}\rho\, V_j(t)^2\, C_{f,j}(\alpha)\, H_j\Delta \tag{12}$$

where the subscript f indicates side or lift component, $F_{f,j}$ is the side or lift force acting on generation point j, ρ is the air density, V_j is the resultant wind velocity dependent on the mean and fluctuating components of the wind, $C_{f,j}(\alpha)$ is the side or lift aerodynamic coefficient dependent on the wind incidence angle α and H_j is the height or width of the wind exposed area at point j for the side or lift force component, respectively, and Δ is the influence length of that point. Regarding the torsional moment M_j imposed by the wind to the deck at the generation point j, this is given by

$$M_j(t) = F_{s,j}(t)\, e_{z,j} + F_{l,j}(t)\, e_{y,j} \tag{13}$$

where $e_{z,j}$ is the vertical eccentricity at the generation point j considering that the vertical coordinate of the centre of pressure is located at half height of the deck and $e_{y,j}$ is the horizontal eccentricity conservatively taken as $B_j/4$ as specified by EN 1991-1-4 (2010). This option was adopted due to the lack of data regarding the moment aerodynamic coefficient of this bridge. However, by using these conservative eccentricities proposed by the norm, the torsional moment obtained through Eq. (13) is higher than that computed using moment aerodynamic coefficients found in the literature for similar box-girder bridges (Zhang et al., 2013; Olmos and Astiz, 2018).

Regarding the vehicle (see Part I for details), the wind load acting on its carbody's centre of gravity may be expressed as

$$F_f(t) = \overline{F_f} + F_f'(t) \tag{14}$$

In which $\overline{F_f}$ is the mean force component given by

$$\overline{F_f} = \frac{1}{2}\rho A\, C_f(\overline{\beta})\, \overline{V_r}^2 \tag{15}$$

and $F_f'(t)$ is the fluctuating component defined as

$$F_f^{'}(t) = \rho\, A\, C_f(\overline{\beta})\, \overline{U} \left(1 + \frac{1}{2C_f(\overline{\beta})}\, C_f^{'}(\overline{\beta})\, \cot\overline{\beta}\right) \int_0^{\infty} h_F(\tau)\, u(t-\tau) d\tau \qquad (16)$$

where the subscript f indicates side or lift component, $\overline{U}$ is the mean wind velocity, A is the reference area, $C_f(\overline{\beta})$ and $C_f^{'}(\overline{\beta})$ are the side or lift aerodynamic coefficients and respective derivatives evaluated at the mean yaw angle $\overline{\beta}$, $\overline{V_r}$ is the mean relative velocity and $h_F(\tau)$ is a weighting function to overcome the limitations of the quasi-steady theory related to the fact that the fluctuating wind force does not strictly follows the turbulent component of the wind. These expressions are also used to obtain the overturning moment $M_v(t)$, but considering AH instead of A, where H is the reference height, and the appropriate aerodynamic coefficient. Note that, according to several studies (Suzuki et al., 2003; Bocciolone et al., 2008; Cheli et al., 2010), for yaw angles lower than 40°, which is always fulfilled in all the analyses considered in this work, the aerodynamic properties of the vehicles are not considerably sensitive to the surrounding configuration, i.e., the aerodynamic coefficients when the vehicle is located over a viaduct or over flat ground are similar (Cheli et al., 2010). Therefore, the aerodynamic coefficients present in the Annex C of EN 14067-6 (2016) relative to a standard ground configuration were adopted in this work.

3.2. Bridge, track and train models

The present paper is not restricted to evaluate the traffic stability in the particular case of the Arroyo de Las Piedras viaduct, but also to draw more general conclusions regarding the influence of other factors in the passenger riding comfort. Hence, with respect to the viaduct, the same parametrization shown in Part I (Montenegro et al., 2022) to consider different lateral flexibilities has also been adopted here to check if this factor influences the riding comfort against lateral winds. This parametrization resulted in four different models (see Table 5) made from the original high-pier steel-composite viaduct composed by 19 continuous spans of 50.4 + 17 × 63.5 + 44 + 35 m (see Part I for a detailed description of the Arroyo de Las Piedras viaduct and the parametrization process)

The FEM model of the viaduct has been developed in ANSYS® (2018) through beam finite elements to model the deck, piers and rails, spring-dashpots to model the ballast and fastener behaviour in the track and discrete mass points to model non-structural masses, such as the ballast, and localized elements, such as the pier diaphragms. Regarding the track irregularities and vehicle, the four levels of track condition (none, low, medium and high levels for HS railways defined by Claus and Schiehlen (1998)) and the Spanish AVE-103 HS train used for the running safety study presented in Part I (Montenegro et al., 2022), have been used in all the dynamic analyses.

3.3. Coupling formulation

The TTBI model used to assess the vehicle's behaviour has already been briefly described in Part I of this paper (Montenegro et al., 2022), while the full mathematical formulation and its validation is presented in previous publications from the authors (Montenegro et al., 2013, 2015; Neves et al., 2014) and successfully applied in distinct contexts within the authors' research group (Montenegro et al., 2016; Heleno et al., 2021; Neto et al., 2021; Neves et al., 2021; Peixer et al., 2021). The TTBI tool relies on a wheel-rail contact model that takes into consideration the shape of the contacting bodies and computes the normal and tangential forces using the Hertz nonlinear law and the Kalker's USETAB algorithm, respectively. To couple the train to the track-bridge system, the governing equilibrium equation of motion of both sub-systems are complemented with constraint equations that connect them. The whole algorithm is programmed in MATLAB® (2018), which carries out the dynamic analysis. However, before doing so, the TTBI tool imports the structural matrices from both the vehicle and track-bridge systems, previously modelled in a FEM package (in this case ANSYS® (2018)).

Table 5
Studied scenarios based on the lateral flexibility of the corresponding structural model.

Scenario i	Description	Relative flexibility $\Delta\delta_i$(%)
S1	Rigid viaduct	0
S2	Medium flexibility	50
S3	Original viaduct (high flexibility)	100
S4	Very high flexibility	150

4. Riding comfort analysis: results and discussion

4.1. Overview of the analysis

The riding comfort evaluation performed in this work has been carried out based on the European and Sperling methods described before. To achieve the comfort indexes, the main inputs consist of the accelerations in the vehicle's carbody obtained numerically through TTBI analysis considering different train speeds (between 140 km/h up to 420 km/h), wind mean velocities (between 20 m/s to 30 m/s), structural lateral conditions (parameterization of the original Arroyo de Las Piedras viaduct) and track qualities (perfect condition and three levels of irregularities). The wind fields used here, as well as the conditions of its application to the train-track-bridge system (maximum gust occurs at the midpoint of the bridge), are the same as those presented in Montenegro et al. (2022) evaluate running safety.

The riding comfort is evaluated not only for a single case study, but for a range of conditions that allow to draw more generic conclusions regarding the traffic stability under wind loads. Therefore, two of the objectives previously discussed regarding train running safety are also addressed here, namely: i) Objective 1: analyse how the riding comfort can be affected by the lateral behaviour of the viaduct when subjected to crosswinds; and ii) Objective 2: analyse the influence of the track condition in the passenger comfort. The analysis of the behaviour of different train types is not addressed here because, unlike the running safety, the riding comfort is highly dependent not only on the vehicle's weight, but also on the other dynamic properties, such as suspension properties, mass distribution, geometry, among others. Therefore, a thorough parametric study on this regard should be carried out first before analysing the riding comfort on specific train types, focusing this work on the analysis of the influence of parameters related with the infrastructure only. Finally, a third objective is also addressed here, which consists of comparing and analysing the results obtained with the European and Sperling methods. By complying with these objectives, the present paper aims to fill a gap in the literature regarding the riding comfort analysis, since all the works in this field, apart from rarely address the comfort on the specific case of bridges and in the presence of crosswinds, are always focused single case studies. Nevertheless, the riding comfort analysis on the original Arroyo de Las Piedras viaduct considering the Spanish AVE-S103 train is firstly addressed in the next subsection.

4.2. Analysis of the actual arroyo de Las Piedras viaduct

4.2.1. Vehicle response

The riding comfort is a sensation dependent on several factors, including the levels of vibrations experienced inside the train. Hence, before presenting the comfort results, it is important to analyse the behaviour of the vehicle in terms of accelerations considering different levels of wind loads and train speeds. Fig. 4 depicts the vertical and lateral accelerations of the carbody for three different wind loads, corresponding to mean wind velocities of 20 m/s, 25 m/s and 30 m/s and a train speed of 300 km/h, while Fig. 5 illustrates the same quantities but for three train speeds, namely 200 km/h, 300 km/h and 400 km/h in the

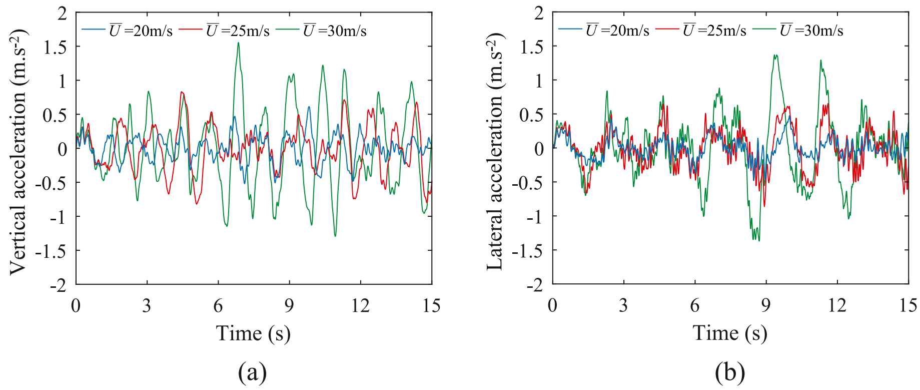

Fig. 4. Accelerations inside the vehicle's carbody for three different wind velocities and for a train speed of 300 km/h: (a) vertical and (b) lateral directions.

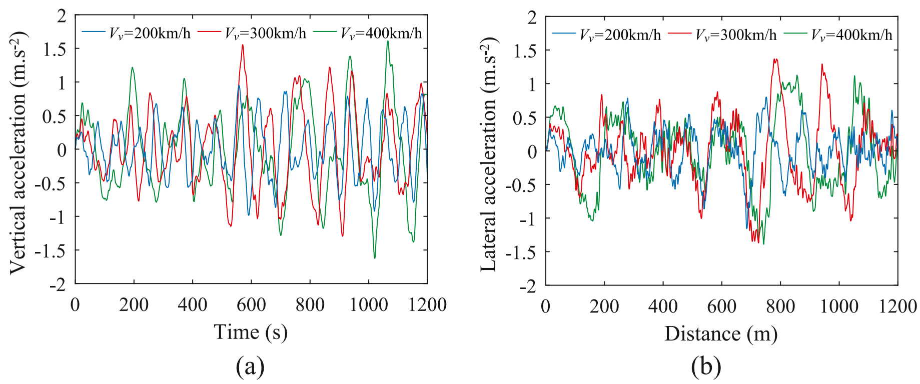

Fig. 5. Accelerations inside the vehicle's carbody for three different train speeds and for a wind mean velocity of 30 m/s: (a) vertical and (b) lateral directions.

presence of a wind field with a mean velocity of 30 m/s (horizontal axis represents the distance covered by the train at different speeds for a more straightforward comparison). All the results within this section correspond to a track condition defined by the high level of irregularities. It is clear that higher wind loads lead to clearly larger vehicle vibrations, both on the vertical and lateral directions. Regarding the train speed, it does not have such a clear effect on the maximum amplitudes of vibrations, since the wind load is clearly dominant over the speed.

4.2.2. Riding comfort analysis

In the present work, the riding comfort is evaluated based on three indexes, namely the Continuous and Mean Comfort indexes specified in the European norm EN 12299 (2009) and the Sperling index present in the Chinese norm GB/T 5599-2019 (2019). As mentioned before, these indexes have been developed to evaluate the comfort throughout a train journey with a considerable length, both in terms of perceived comfort level evaluated through measurements on a long-time (minutes) basis (Mean Comfort) and on a continuous short-time (5-s) basis (Continuous Comfort and Sperling). However, since this work is focused on the riding comfort assessment of HS trains during short periods (the time required to cross a bridge is in the order of seconds), the Mean Comfort index is assessed just for informative purposes. Fig. 6 shows the maximum values of the three indexes in the form of isoline maps obtained in each dynamic analysis characterized by each wind velocity/train speed pair, considering the so-called base scenario, i.e., original viaduct model, AVE-S103 HS train and high level of irregularities. By observing the figure, it is possible to conclude that the lateral direction is determinant for the definition of the riding comfort under crosswinds according to the European method, since the Continuous Comfort index in this direction is higher than that obtained for the vertical direction. However, the opposite is observed when evaluating the riding comfort through the Sperling method. This is due to the relation between the frequency sensitive ranges adopted on both indexes and the natural frequencies of the main vibration modes of the vehicle's carbody. To support this conclusion, Fig. 7 depicts the main modes of vibration of the carbody, and respective natural frequencies, together with the graphic of weighting functions previously shown but enhancing the frequencies of interest. It is possible to observe that the natural frequencies of both lateral and vertical vibration modes of the carbody are always within 0.5 Hz and 1.1 Hz, while the frequency sensitive ranges associated with the Sperling index on both directions and with the Continuous index for the vertical direction are significantly above this interval ([3, 7] Hz for W_{Zy} and W_{Zz} and [4, 16.5] Hz for C_{Cz}). The same is not true when looking to the sensitive range for the Continuous index for the lateral direction (between 0.6 Hz and 2 Hz), which still incorporates part of the frequencies associated with the natural vibrations of the vehicle's carbody. As a result, the frequency weighting function associated with this last index has a lower impact in the weighted amplitude of the accelerations (weight factor ≈1.0) when compared to the other indexes (weight factors ranging between 0.4 and 0.6).

To better illustrate the aforementioned conclusion, Fig. 8 compares the original responses of the carbody with the corresponding weighted responses obtained with the European and Sperling frequency weighting functions. The responses, which are depicted on both time and frequency domain, correspond to a scenario with mean wind velocity of 30 m/s and train speed of 300 km/h. When looking to the results obtained with the European method, it is clear that the lateral filter has a much lower impact in the amplitude of the weighted response when compared to the vertical one, which cuts its amplitude in more than a half. This is in accordance with the weights associated with the carbody natural frequencies shown previously in Fig. 7.a. For the Sperling method, however, the weighting filters affect the vertical and lateral responses in similar ways, which justifies the lower differences between the indexes on both directions presented in Fig. 6d and 6.e. This was already

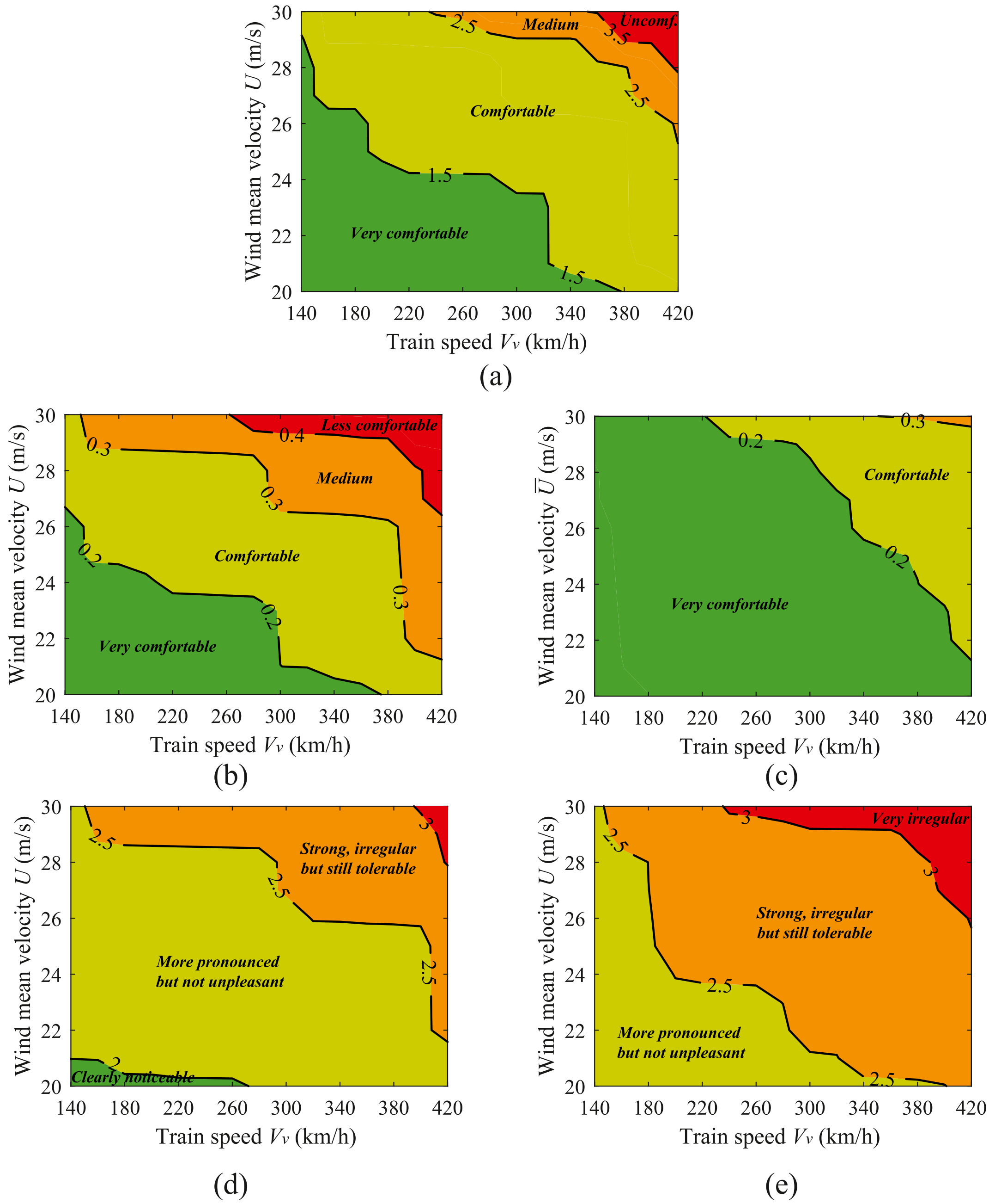

Fig. 6. Maximum values of the riding comfort indexes: (a) N_{MV}, (b) C_{Cy}, (c) C_{Cz}, (d) W_{Zy} and (e) W_{Zz}.

notorious in the weight factors associated with the carbody natural frequencies previously depicted in Fig. 7.b.

4.3. Passenger comfort depending on the lateral flexibility of the viaduct

Crosswinds may cause significant levels of vibration to the bridges, especially in the lateral direction. However, it is not guaranteed that these vibrations will affect the behaviour of the vehicle in terms of carbody's accelerations and, consequently, the passenger comfort. Thus, to help understand the influence of the lateral behaviour of a viaduct in the passenger riding comfort when it is subjected to lateral winds, Fig. 9 illustrates the maximum values of the comfort indexes obtained with the original viaduct model (Scenario S3, see Table 5, solid lines) and with the rigid one (Scenario S1, see Table 5, dashed line) for a situation without wind and for two winds scenarios characterized by mean wind velocities of 20 m/s and 30 m/s (AVE-S103 HS train and a track quality characterized by the high level of irregularities). Due to the reason stated above, and due to space limitations, the Mean Comfort index is not addressed hereafter. It can be observed that the differences between the purely rigid structural model and the flexible viaduct are relatively small, showing that the model's lateral flexibility does not meaningfully affect the results. The exceptions are the indexes relative to the vertical direction, especially the Sperling, when no wind is considered in the analysis, because in these situations the vertical interaction between the bridge and vehicle interfere with the latter's vertical response. However, in the presence of crosswinds, the wind load becomes predominant for the vehicle's response when compared to the vehicle-bridge interaction effects caused by the movement of the structure. Once more, note that the lateral direction is determinant when adopting the European code method, while for the Sperling method the differences between the indexes on the two directions are not so significant.

To emphasize the aforementioned conclusion, Fig. 10 plots the

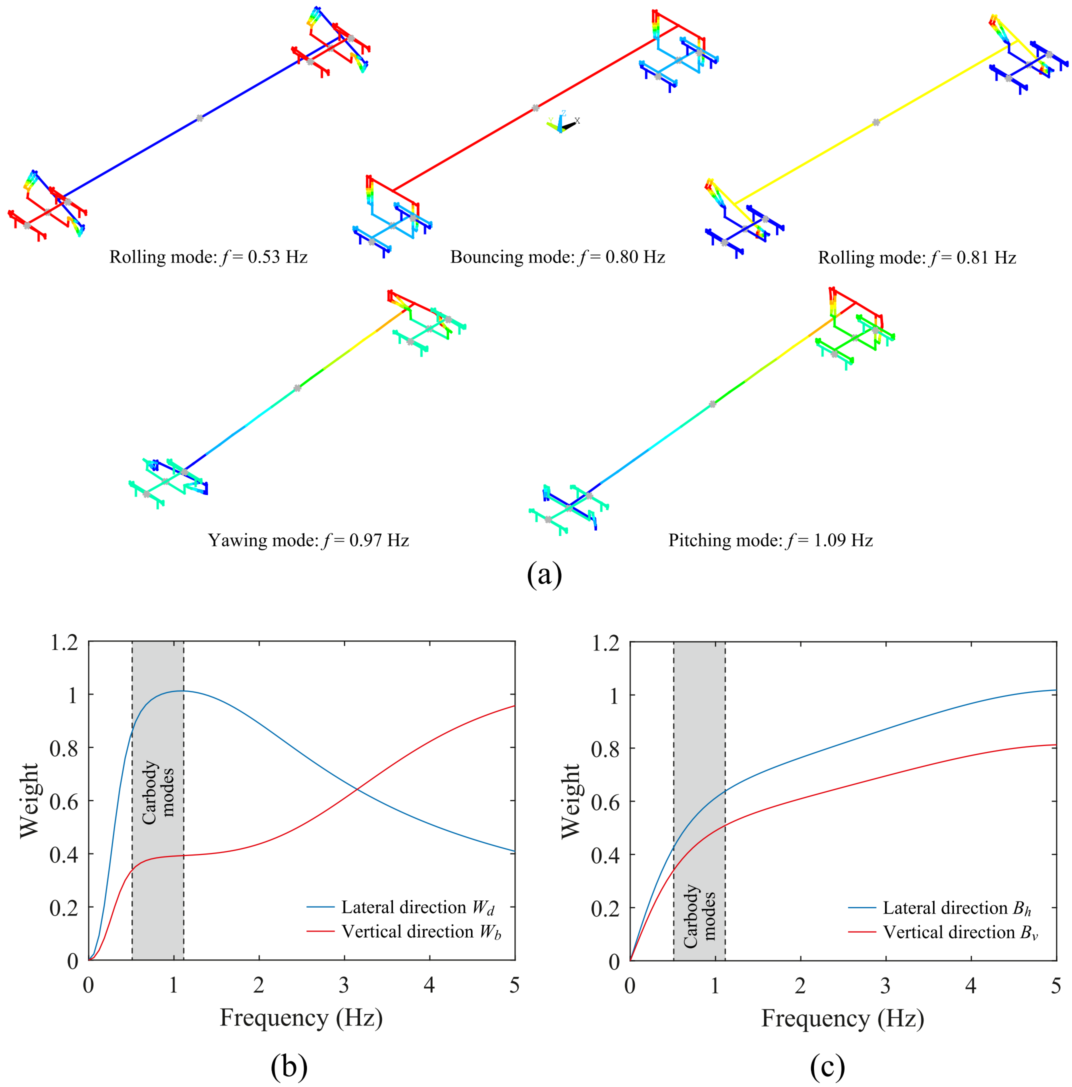

Fig. 7. Relation between carbody's vibration modes and frequency sensitive ranges of the indexes: (a) natural modes of vibration of the carbody and weighting factors of the (b) Continuous Comfort and (c) Sperling indexes.

vertical and lateral accelerations inside the carbody considering the four flexibility scenarios described in Table 5 for a train speed of 300 km/h and a crosswind with mean wind velocity of 30 m/s. As expected, both the vertical and lateral responses of the vehicle are not significantly affected by the viaduct's lateral behaviour against the wind load. As explained before, although the viaduct's behaviour is significantly different (larger lateral movements as the flexibility increases) the vehicle's response is mainly controlled by the wind that is acting directly on it. This effect has been previously observed in Part I of this paper (Montenegro et al., 2022), but in relation to the running safety.

Finally, the maximum values of the Continuous Comfort and Sperling indexes obtained in all the dynamic analyses performed in this study for the four flexibility scenarios described in Table 5 and considering the base traffic situation (AVE-S103 HS train and a track quality characterized by the high level of irregularities) are plotted in Fig. 11. Since the comfort may be controlled by both directions, these isoline graphics represent the maximum values of the comfort indexes between the vertical and lateral directions. Generally, the four scenarios exhibit similar values of the comfort indexes, meaning that, as for the running safety (Montenegro et al., 2022), the lateral behaviour of the viaduct does not meaningfully affect the results in the presence of crosswinds. When comparing the Continuous Comfort and Sperling indexes, although the scales are not the same, a general equivalency between them is observed, i.e., the comfort levels start to be unpleasant for similar wind and train speed situations. Note that, although approximately coincident, the isolines obtained with the four models differ slightly in some points but without a specific trend, i.e., the critical model is not always the same. However, since the differences are small, these random differences may be explained by the stochastic nature of the wind and track irregularities.

Finally, it is important to stress that this study only shows that the lateral behaviour of the viaduct does not significantly influence the carbody's vibrations, since the wind that is acting on the vehicle is determinant. However, in some bridges prone to resonant effects caused by the train passage, such as those composed by simply supported spans, the vehicle's carbody may experience amplifications in the vertical vibrations related with the vehicle-bridge coupling, which may influence the passenger comfort. Nevertheless, since the bridges are designed to guarantee that these effects do not condition the train's operation, it is unlikely that they may become more predominant than the wind load. For this reason, the conclusions drawn here may be considered generic, i.e., the structural behaviour has a smaller influence in the passenger comfort when compared with the effects caused by strong crosswinds.

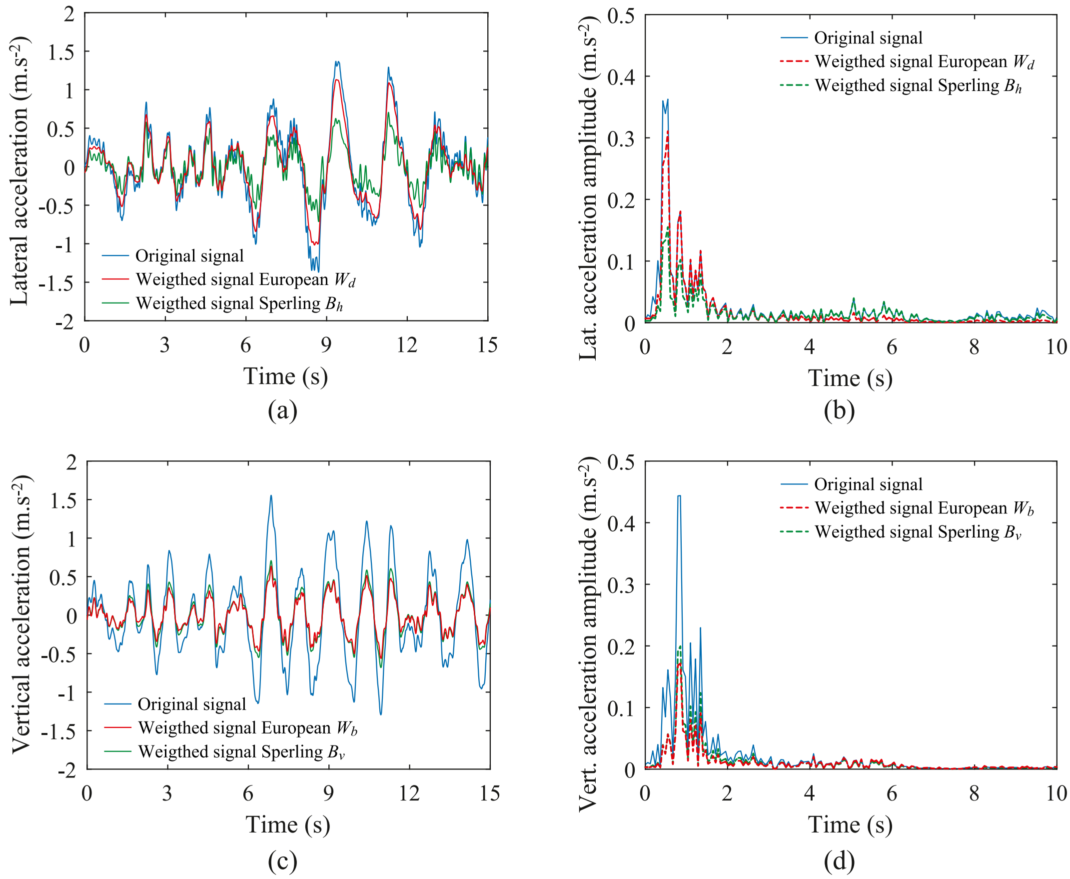

Fig. 8. Comparison between the original response of the carbody and the corresponding weighted responses according to the European and Sperling methods: lateral direction in the (a) time and (b) frequency domain and vertical direction in the (c) time and (d) frequency domain.

4.4. Passenger comfort depending on the track maintenance condition

As in the previous section, Fig. 12 plots the maximum values of the comfort indexes for three wind scenarios ($\overline{U} = 0$ m/s, $\overline{U} = 20$ m/s and $\overline{U} = 30$ m/s) considering a situation with the high level of irregularities (solid lines) and with a theoretical perfect track (dashed lines). All the analyses have been performed considering the flexible model of the original viaduct (Scenario S3, see Table 5) and the AVE-S103 HS train. When looking to the results, generally, the level of irregularities considered in this work does not significantly affect the comfort level in the wind scenarios, since the wind load is much more determinant for the carbody vibrations than the track condition. However, note that only admissible levels of irregularities for HS railways have been used in the analyses (the amplitude of the deviations are still far from the limits defined in EN 13848-5 (2005)), which contributes to the lower influence of this factor to the carbody's vibration. Without the presence of wind, the irregularities are more notorious, especially in the lateral Sperling index W_{zy}. Curiously, in the vertical direction, the differences in the W_{zz} are much lower, since the vertical flexibility of the viaduct is conditioning the vehicle's vibrations more significantly than the vertical irregularities themselves. To justify this conclusion, Fig. 13 illustrates the maximum vertical comfort indexes for the analysis without wind but considering the rigid (Scenario S1) and flexible (Scenario S3) scenarios with and without track irregularities. By looking to the figure, it is possible to observe that, for both indexes, the differences between the levels of comfort with and without irregularities are much more pronounced in the rigid scenario, as there are no vertical vibrations of the viaduct interfering with the vehicle's response. On the other hand, when considering the vertical flexibility of the viaduct, its vertical response affects the vehicle's behaviour, which camouflages the influence of the track irregularities.

To conclude, the results obtained for all the wind loads, as well as for the remaining track conditions (low and medium levels) are summarized in the isoline maps depicted in Fig. 14. As in the previous section, the graphics combine the maximum values of the lateral and vertical indexes and are related with the base scenario (AVE-S103 HS train and flexibility scenario S3, i.e., the original viaduct). The results corroborate the preliminary findings shown, i.e., the influence of the wind load is determinant to the riding comfort when compared to the levels of track condition considered here. Since the only situations where the irregularities conditioned the passenger comfort are not plotted in these graphs (windless scenarios without considering the bridge's flexibility as shown in Fig. 13), all the isolines are practically coincident. Nonetheless, it is important to stress once again that only allowable track irregularities for HS are considered here. Poorer track conditions are not addressed since it would result in unrealistic HS railways scenarios.

5. Conclusions

This work consists of the second part of a paper that aims to evaluate the impact of the train-track-bridge system characteristics in the riding behaviour of HS trains when crossing bridges subjected to crosswinds. While Part I addresses the running safety of trains moving over bridges under wind conditions, this Part II aims to investigate the effects of the wind loads in the passenger riding comfort. This study evaluates the riding comfort against crosswind not only in a unique train-bridge scenario, but also considering different situations by performing parametric dynamic analyses through the variation of the train speed, wind velocity, bridge's lateral behaviour and track condition. The riding comfort has been evaluated based on three indexes, namely the Mean and

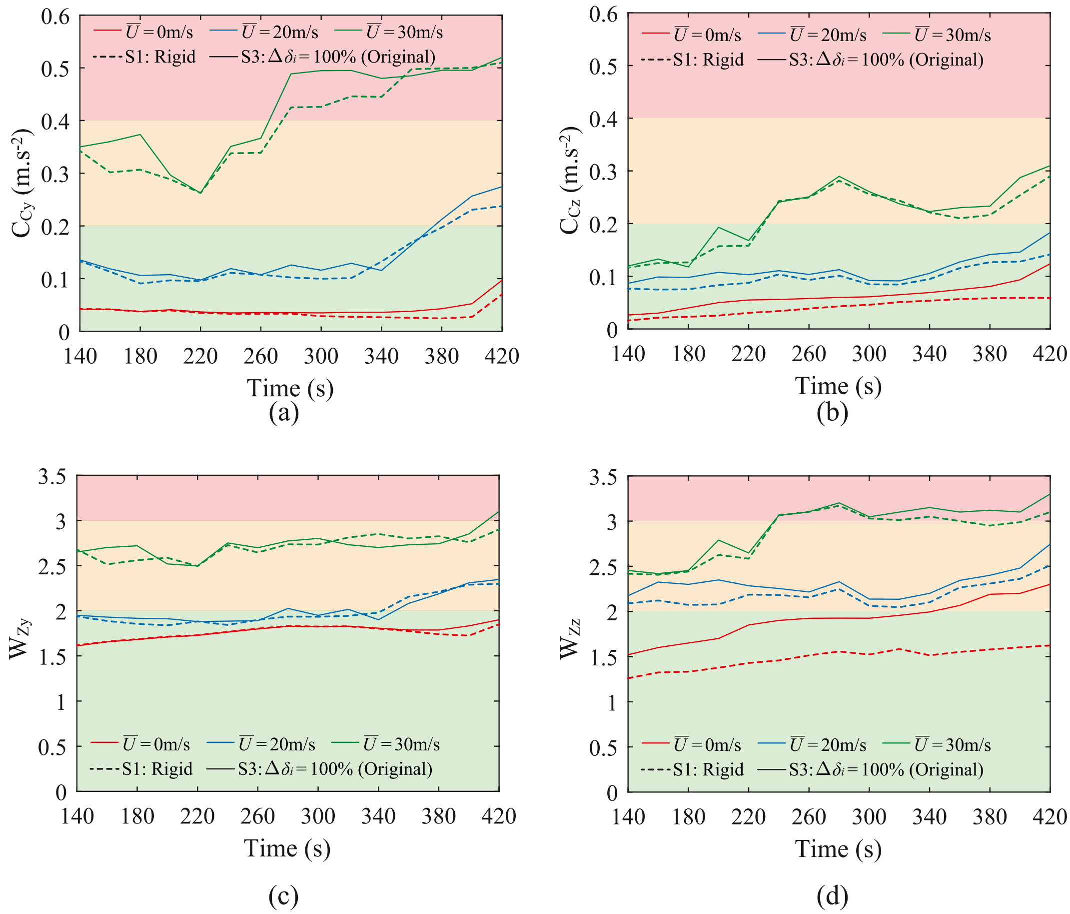

Fig. 9. Maximum comfort indexes obtained with the flexible viaduct model (Scenario S3) and the rigid one (Scenario S1) considering three wind scenarios: (a) C_{Cy}, (b) C_{Cz}, (c) W_{Zy} and (d) W_{Zz}.

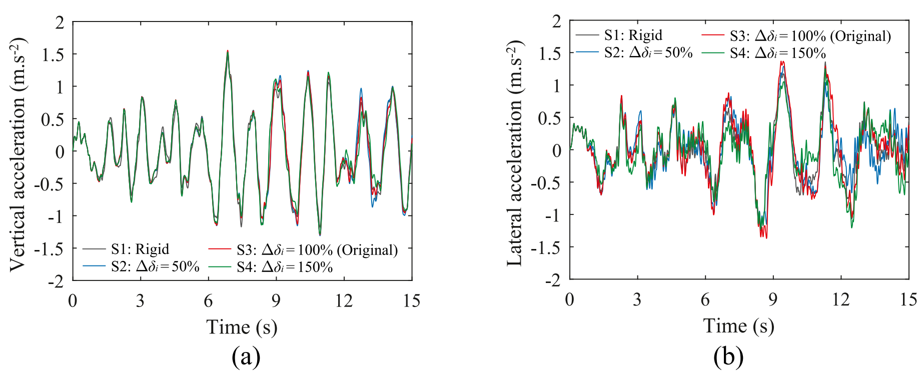

Fig. 10. Vibrations experienced inside the carbody considering the four flexibility scenarios, a wind field characterized by $\overline{U} = 30$ m/s and a train speed of 300 km/h: (a) vertical and (b) lateral accelerations.

Continuous Comfort indexes, stipulated in the European Norm EN 12299, and the Sperling index, adopted in the Chinese norm GB/T 5599-2019.

Three main objectives were stipulated in this paper regarding the analysis of the riding comfort on bridges in the presence of crosswinds: i) impact of the bridge's lateral structural response; ii) influence of the track considering admissible levels of irregularities for HS railways; iii) analyse different methodologies to evaluate the riding comfort, namely the European and Sperling methods. By answering to these goals, this paper brought new findings regarding a topic that is still understudied by the main researchers in this field. Thus, the following conclusions can be drawn:

- In a preliminary analysis of the vehicle response running on the actual Arroyo de Las Piedras viaduct in the presence of crosswinds, it has been demonstrated that the wind velocity has a strong impact in the vehicle's lateral and vertical response. Regarding the train speed, it does not have such a clear effect on the vehicle's response in the presence of crosswinds, since the wind load is clearly dominant.
- Regarding the riding comfort analysis itself, the results show that the levels of vibrations become less tolerable only for high train speeds and wind loads. Interesting conclusions are also drawn when the European and Sperling methods are compared. While the comfort index defined by the former is mainly conditioned by the lateral direction, the latter is also controlled by the vertical vibrations. Such

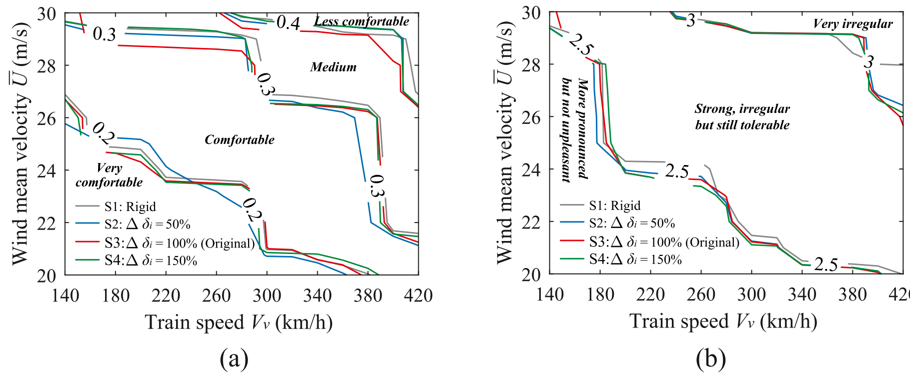

Fig. 11. Maximum values of the riding comfort indexes: (a) max(C_{Cy}, C_{Cz}) and (b) max(W_{Zy}, W_{Zz}).

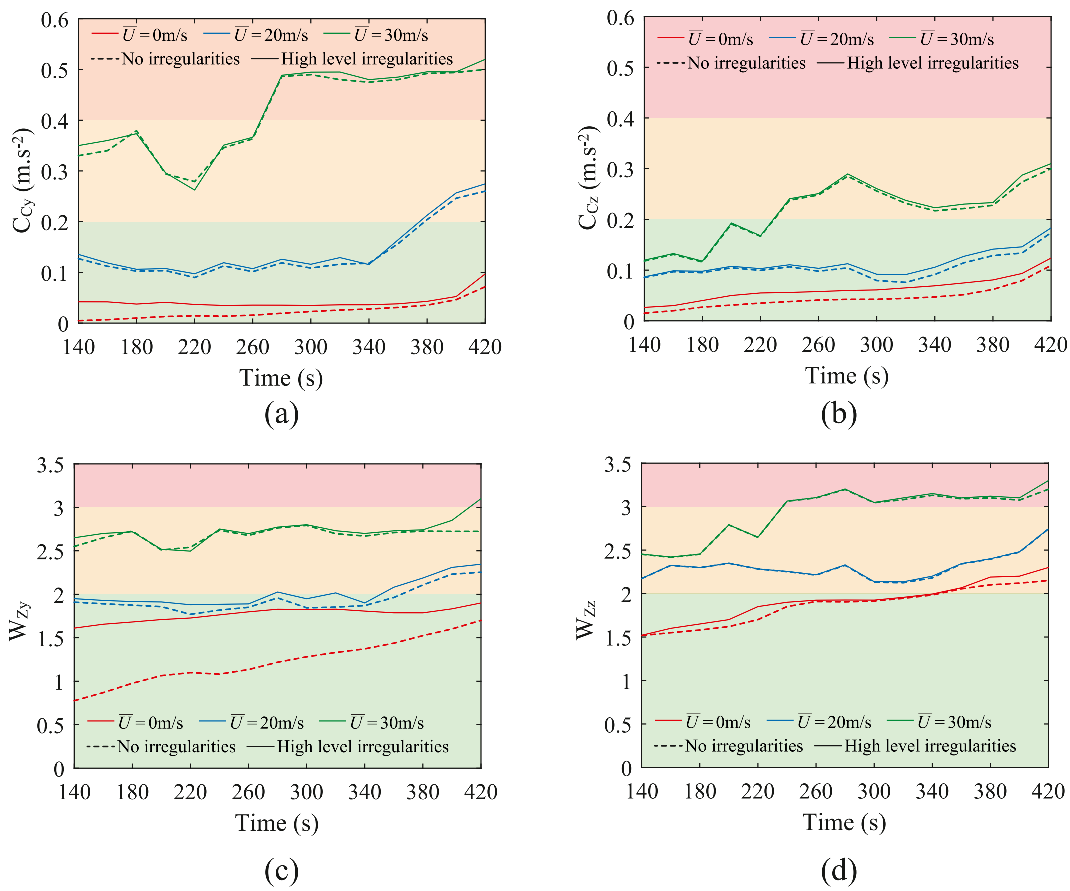

Fig. 12. Maximum comfort indexes obtained with and without irregularities considering three wind scenarios: (a) C_{Cy}, (b) C_{Cz}, (c) W_{Zy} and (d) W_{Zz}.

phenomenon is justified by the fact that the weighting function adopted by the European method to analyse the lateral vibrations is characterized by frequencies of interest close to those typically associated to the main vibration modes of the carbody of a railway vehicle (between 0.5 Hz and 1.5 Hz).

- The lateral behaviour of the viaduct when subjected to lateral wind loads have a small impact in the vibrations of the carbody and, consequently, in the passenger riding comfort. The results demonstrate that, although the more flexible bridges tend to have a much more pronounced level of lateral vibrations, as demonstrated in Part I, the impact in the comfort indexes is not meaningful. This means that the wind load acting on the vehicle itself is dominant for the carbody's vibration when compared to the effects transmitted by the lateral movement of the bridge. Moreover, although the scales adopted by both indexes are different, the comfort levels estimated by the Continuous Comfort and Sperling indexes are somehow equivalent, with pleasant and unpleasant levels of vibration associated to the same wind and train speed situations.
- The last part of this study consisted of the evaluation of the influence of the track condition in the passenger riding comfort in the presence of crosswinds. The results demonstrate that, for the levels of irregularities considered here, which are all within the admissible levels for HS railways, the influence of the wind load in the vehicle's response is once again determinant, leading to small differences in the comfort indexes when considering different condition levels.

This two-part paper aims to demonstrate the influence of several factors in the runnability of HS train moving over bridges subjected to

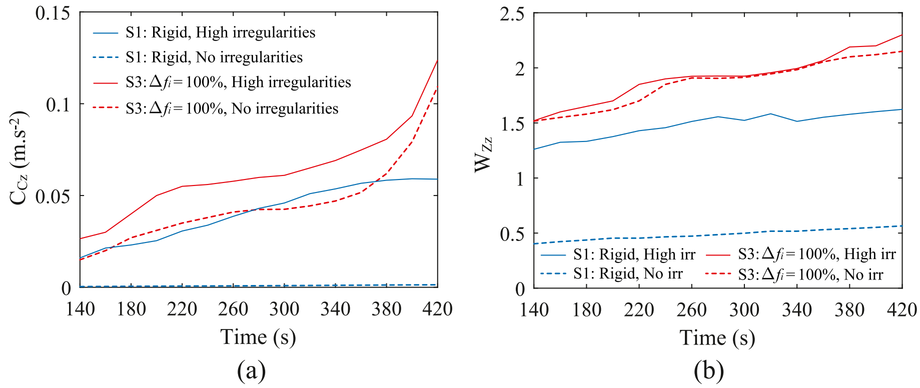

Fig. 13. Maximum vertical comfort indexes obtained with and without irregularities considering the flexible viaduct model (Scenario S3) and the rigid one (Scenario S1) for $\overline{U} = 0$ m/s: (a) C_{Cz}, (b) W_{Zz}.

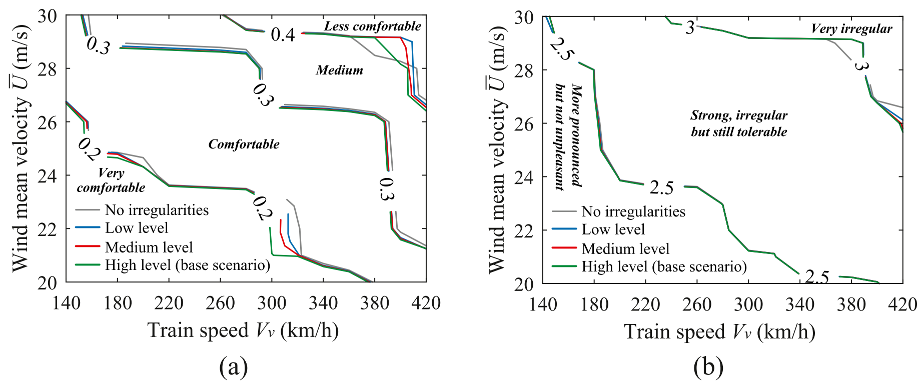

Fig. 14. Maximum values of the riding comfort indexes: (a) max(C_{Cy}, C_{Cz}) and (b) max(W_{Zy}, W_{Zz}).

crosswinds. The authors expect that the conclusions drawn here may be used by other researchers to guide their future work in this field and, at the same time, by designers of HS railway bridges, whose concerns regarding safety and comfort are usually critical for decision-making.

CRediT authorship contribution statement

P.A. Montenegro: Conceptualization, Methodology, Software, Validation, Investigation, Writing – original draft, Writing – review & editing, Supervision. **D. Ribeiro:** Methodology, Investigation, Writing – review & editing. **M. Ortega:** Resources, Formal analysis. **F. Millanes:** Resources. **W. Zhai:** Investigation, Writing – review & editing, Formal analysis, Methodology, Writing – review & editing. **R. Calçada:** Writing – review & editing, Visualization, Funding acquisition.

Declaration of competing interest

The authors declare that they have no known competing financial interests or personal relationships that could have appeared to influence the work reported in this paper.

Acknowledgements

This work was financially supported by: Base Funding - UIDB/04708/2020 and Programmatic Funding - UIDP/04708/2020 of the CONSTRUCT - Instituto de I&D em Estruturas e Construções - funded by national funds through the FCT/MCTES (PIDDAC); Grant no. 2020.00305. CEECIND from the Stimulus of Scientific Employment, Individual Support (CEECIND) - 3rd Edition provided by "FCT–Fundação para a Ciência e Tecnologia".

References

ANSYS®, 2018. Academic Research, Release, 19.2. ANSYS Inc., Canonsburg, PA, USA.

Antolin, P., Goicolea, J.M., Astiz, M.A., 2012. Chapter 6: strategies for modeling train-bridge lateral dynamic interaction. In: Xia, H., De Roeck, G., Goicolea, J.M. (Eds.), Bridge Vibration and Controls: New Research. Nova Science Publishers, Inc, New York City, NY, USA.

Bocciolone, M., Cheli, F., Corradi, R., Muggiasca, S., Tomasini, G., 2008. Crosswind action on rail vehicles: wind tunnel experimental analyses. J. Wind Eng. Ind. Aerod. 96 (5), 584–610. https://doi.org/10.1016/j.jweia.2008.02.030.

Cao, Y., Xiang, H., Zhou, Y., 2000. Simulation of stochastic wind velocity field on long-span bridges. J. Eng. Mech. 126 (1), 1–6. https://doi.org/10.1061/(ASCE)0733-9399(2000)126:1(1).

Cheli, F., Corradi, R., Rocchi, D., Tomasini, G., Maestrini, E., 2010. Wind tunnel tests on train scale models to investigate the effect of infrastructure scenario. J. Wind Eng. Ind. Aerod. 98 (6–7), 353–362. https://doi.org/10.1016/j.jweia.2010.01.001.

Claus, H., Schiehlen, W., 1998. Modeling and simulation of railway bogie structural vibrations. Veh. Syst. Dyn. 29 (1), 538–552. https://doi.org/10.1080/00423119808969585.

Deng, C., Zhou, J., Thompson, D., Gong, D., Sun, W., 2021. Analysis of the consistency of the Sperling index for rail vehicles based on different algorithms. Veh. Syst. Dyn. 59 (2), 313–330. https://doi.org/10.1080/00423114.2019.1677923.

Dumitriu, M., Leu, M., 2017. Correlation between ride comfort index and sperling's index for evaluation ride comfort in railway vehicles. Appl. Mech. Mater. 880, 201–206. https://doi.org/10.4028/www.scientific.net/AMM.880.201.

EN 1991-1-4, 2010. Eurocode 1: Actions on Structures - Part 1-4: General Actions - Wind Actions. CEN, Brussels.

EN 12299, 2009. Railway Applications - Ride Comfort for Passengers - Measurement and Evaluation. CEN, Brussels.

EN 13848-5, 2005. Railway Applications - Track - Track Geometry Quality - Part 5: Geometric Quality Assessment. CEN, Brussels.

EN 14067-6, 2016. Railway Applications - Aerodynamics - Part 6: Requirements and Test Procedures for Cross Wind Assessment. CEN, Brussels.

GB/T 5599-2019, 2019. Specification for dynamic performance assessment and testing verification of rolling stock. In: People's Republic of China National Railway Administration (CNRA-PRC), Beijing.

Gong, D., Gu, W.J., Zhou, J.S., 2013. Study on geometry filtering phenomenon and flexible car body resonant vibration of articulated trains. Adv. Mater. Res. 787, 542–547. https://doi.org/10.4028/www.scientific.net/AMR.787.542.

Guo, W.W., Xia, H., Zhai, N., 2013. Dynamic responses of tsing Ma bridge and running safety of trains subjected to typhoon york. Int. J. Rail. Transp. 1 (3), 181–192. https://doi.org/10.1080/21650349.2013.808417.

Guo, W.W., Xu, Y.L., Xia, H., Zhang, W.S., Shum, K.M., 2007. Dynamic response of suspension bridge to typhoon and trains. II: numerical results. J. Struct. Eng. 133 (1), 12–21. https://doi.org/10.1061/(ASCE)0733-9445(2007)133:1(12).

He, X., Gai, Y., Wu, T., 2017. Simulation of train–bridge interaction under wind loads: a rigid-flexible coupling approach. Int. J. Rail. Transp. 6 (3), 163–182. https://doi.org/10.1080/23248378.2017.1415170.

Heleno, R., Montenegro, P.A., Carvalho, H., Calçada, R., Baker, C.J., 2021. Influence of the railway vehicle properties in the running safety against crosswinds. J. Wind Eng. Ind. Aerod. 217, 104732. https://doi.org/10.1016/j.jweia.2021.104732.

ISO 2631-4, 2001. Mechanical Vibration and Shock - Evaluation of Human Exposure to Whole Body Vibration - Part 4: Guidelines for the Evaluation of the Effects of Vibration and Rotational Motion on Passenger and Crew Comfort in Fixed Guideway Transport Systems. ISO, Geneve.

Jiang, Y., Chen, B.K., Thompson, C., 2019. A comparison study of ride comfort indices between Sperling's method and EN 12299. Int. J. Rail. Transp. 7 (4), 279–296. https://doi.org/10.1080/23248378.2019.1616329.

Knothe, K., Stichel, S., 2017. Rail Vehicle Dynamics. Springer International Publishing, Cham, Switzerland. https://link.springer.com/book/10.1007/978-3-319-45376-7.

Kumar, V., Rastogi, V., Pathak, P.M., 2017. Simulation for whole-body vibration to assess ride comfort of a low–medium speed railway vehicle. Simulation: Trans. Soc. Modwl. Simul.Int. 93 (3), 225–236. https://doi.org/10.1177/0037549716679254.

MATLAB®, 2018. Release R2018a. The MathWorks Inc., Natick, MA, USA.

Meixedo, A., Ribeiro, D., Calçada, R., Delgado, R., 2014. Global and local dynamic effects on a railway viaduct with precast deck. In: Railways 2014 - 2nd International Conference on Railway Technology: Research, Development and Maintenance. Civil-Com Press, Ajaccio, France.

Montenegro, P.A., Barbosa, D., Carvalho, H., Calçada, R., 2020a. Dynamic effects on a train-bridge system caused by stochastically generated turbulent wind fields. Eng. Struct. 211, 1–16. https://doi.org/10.1016/j.engstruct.2020.110430.

Montenegro, P.A., Calçada, R., Vila Pouca, N., Tanabe, M., 2016. Running safety assessment of trains moving over bridges subjected to moderate earthquakes. Earthq. Eng. Struct. Dynam. 45, 483–504. https://doi.org/10.1002/eqe.2673.

Montenegro, P.A., Carvalho, H., Ortega, M., Millanes, F., Goicolea, J.M., Zhai, W.M., Calçada, R., 2022. Impact of the train-track-bridge-wind system characteristics in the runnability of high-speed trains against crosswinds - Part I: running safety. J. Wind Eng. Ind. Aerod. 224, 104974. https://doi.org/10.1016/j.jweia.2022.104974.

Montenegro, P.A., Carvalho, H., Ribeiro, D., Calçada, R., Tokunaga, T., Tanabe, M., Zhai, W., 2021. Assessment of train running safety on bridges: a literature review. Eng. Struct. 241, 112425. https://doi.org/10.1016/j.engstruct.2021.112425.

Montenegro, P.A., Heleno, R., Carvalho, H., Calçada, R., Baker, C.J., 2020b. A comparative study on the running safety of trains subjected to crosswinds simulated with different wind models. J. Wind Eng. Ind. Aerod. 207, 104398. https://doi.org/10.1016/j.jweia.2020.104398.

Montenegro, P.A., Neves, S.G.M., Azevedo, A.F.M., Calçada, R., 2013. A nonlinear vehicle-structure interaction methodology with wheel-rail detachment and reattachment. In: COMPDYN 2013 - 4th ECCOMAS Thematic Conference on Computational Methods in Structural Dynamics and Earthquake Engineering, Kos, Greece.

Montenegro, P.A., Neves, S.G.M., Calçada, R., Tanabe, M., Sogabe, M., 2015. Wheel-rail contact formulation for analyzing the lateral train-structure dynamic interaction. Compos. Struct. 152, 200–214. https://doi.org/10.1016/j.compstruc.2015.01.004.

Neto, J., Montenegro, P.A., Vale, C., Calçada, R., 2021. Evaluation of the train running safety under crosswinds - a numerical study on the influence of the wind speed and orientation considering the normative Chinese hat model. Int. J. Rail. Transp. 9 (3), 204–231. https://doi.org/10.1080/23248378.2020.1780965.

Neves, S.G.M., Montenegro, P.A., Azevedo, A.F.M., Calçada, R., 2014. A direct method for analyzing the nonlinear vehicle–structure interaction. Eng. Struct. 69, 83–89. https://doi.org/10.1016/j.engstruct.2014.02.027.

Neves, S.G.M., Montenegro, P.A., Jorge, P.F.M., Calçada, R., Azevedo, A.F.M., 2021. Modelling and analysis of the dynamic response of a railway viaduct using an accurate and efficient algorithm. Eng. Struct. 226, 111308. https://doi.org/10.1016/j.engstruct.2020.111308.

Olmos, J.M., Astiz, M.A., 2018. Improvement of the lateral dynamic response of a high pier viaduct under turbulent wind during the high-speed train travel. Eng. Struct. 165, 368–385. https://doi.org/10.1016/j.engstruct.2018.03.054.

Peixer, M.A., Montenegro, P.A., Carvalho, H., Ribeiro, D., Bittencourt, T., Calçada, R., 2021. Running safety evaluation of a train moving over a high-speed railway viaduct under different track conditions. Eng. Fail. Anal. 121, 105133. https://doi.org/10.1016/j.engfailanal.2020.105133.

Ribeiro, D., Calçada, R., Delgado, R., Brehm, M., Zabel, V., 2012. Finite-element model calibration of a railway vehicle based on experimental modal parameters. Veh. Syst. Dyn. 514 (6), 821–856. https://doi.org/10.1080/00423114.2013.778416.

Suzuki, M., Tanemoto, K., Maeda, T., 2003. The simulation of unsteady aerodynamic cross wind forces on trains. J. Wind Eng. Ind. Aerod. 91 (1–2), 209–218. https://doi.org/10.1016/S0167-6105(02)00346-X.

Wang, M., Li, X., Chen, X., 2021. A Simplified Analysis Framework for Assessing Overturning Risk of High-Speed Trains over Bridges under Crosswind. Vehicle System Dynamics. https://doi.org/10.1080/00423114.2020.1845755 (in press).

Wang, L., Zhang, X., Liu, H., Han, Y., Zhu, Z., Cai, C.S., 2022. Global reliability analysis of running safety of a train traversing a bridge under crosswinds. J. Wind Eng. Ind. Aerod. 224, 104979. https://doi.org/10.1016/j.jweia.2022.104979.

Xiang, H., Tang, P., Zhang, Y., Li, Y., 2020. Random dynamic analysis of vertical train–bridge systems under small probability by surrogate model and subset simulation with splitting. Railway. Eng. Sci. 28 (3), 305–315. https://doi.org/10.1007/s40534-020-00219-6.

Xu, Y.L., Guo, W.W., Chen, J., Shum, K.M., Xia, H., 2007. Dynamic response of suspension bridge to typhoon and trains. I: field measurement results. J. Struct. Eng. 133 (1), 3–11. https://doi.org/10.1061/(ASCE)0733-9445(2007)133:1(3).

Zhai, W., Han, Z., Chen, Z., Ling, L., Zhu, S., 2019. Train–track–bridge dynamic interaction: a state-of-the-art review. Veh. Syst. Dyn. 57 (7), 984–1027. https://doi.org/10.1080/00423114.2019.1605085.

Zhang, T., Xia, H., Guo, W.W., 2013. Analysis on running safety of train on bridge with wind barriers subjected to cross wind. Wind Struct. 17 (2), 203–225. https://doi.org/10.12989/was.2013.17.2.203.